



## Synthesis and structure–activity relationships of novel benzofuran farnesyltransferase inhibitors

Kohsuke Asoh, Masami Kohchi, Ikumi Hyoudoh, Tatsuo Ohtsuka, Miyako Masubuchi, Kenichi Kawasaki, Hiroshiro Ebiike, Yasuhiko Shiratori, Takaaki A. Fukami, Osamu Kondoh, Toshiyuki Tsukaguchi, Nobuya Ishii, Yuko Aoki, Nobuo Shimma, Masahiro Sakaitani\*

Kamakura Research Laboratories, Chugai Pharmaceutical Co. Ltd., 200-Kajiwara, Kamakura, Kanagawa 247-8530, Japan

### ARTICLE INFO

#### Article history:

Received 28 July 2008

Revised 21 January 2009

Accepted 23 January 2009

Available online 11 February 2009

#### Keywords:

Farnesyltransferase inhibitors

Anti cancer

Tipifarnib

Benzofuran

### ABSTRACT

A series of benzofuran-based farnesyltransferase inhibitors have been designed and synthesized as anti-tumor agents. Among them, **11f** showed the most potent enzyme inhibitory activity ( $IC_{50} = 1.1$  nM) and antitumor activity in human cancer xenografts in mice.

© 2009 Published by Elsevier Ltd.

Membrane-bound GTP binding proteins (G-proteins) act as molecular switches to regulate cell growth by cycling between the inactive GDP-bound state and the active GTP-bound state. In tumor cells, the constitutive activation of some G-proteins contributes to their malignant growth properties. In normal cells, this switching mechanism is highly regulated and G-proteins are found predominantly in their inactive GDP-binding state. All of these G-proteins originally have the CAAX tetrapeptide motif (C: Cys, A: an aliphatic amino acid, X: Ser, Met, Gln, Ala) at their C-terminal.<sup>1</sup> Farnesyltransferase (FTase) enzymes recognize this CAAX tetrapeptide motif and transfer the farnesyl group to the cysteine thiol. This farnesylation is critical for membrane binding and the biological function of G-proteins.<sup>2</sup> In the last decade, many classes of FTase inhibitors have been reported and discussed as antitumor agents.<sup>3</sup> Tipifarnib (R115777) is one of the most potent FTase inhibitors that is undergoing clinical trials.<sup>4</sup> In order to discover new potent FTase inhibitors, we searched for a novel core template in place of the quinolinone moiety of tipifarnib. The first templates, 4-substituted phenyl rings **1** and bicyclic structures **2** such as benzofuran and benzothiophene, displayed moderate FTase inhibition but no antiproliferative activity against tumor cells. Further modification studies resulted in the second templates, the biaryl series **3** which showed weak activity against both FTase and tumor cells. We report herein our design and synthesis of the series of benzo-

furan FTase inhibitors **4** using the X-ray structure of human FTase. (Fig. 1).

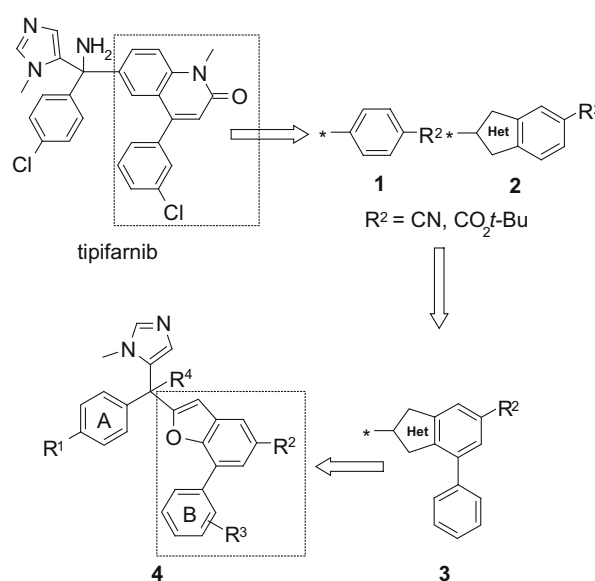
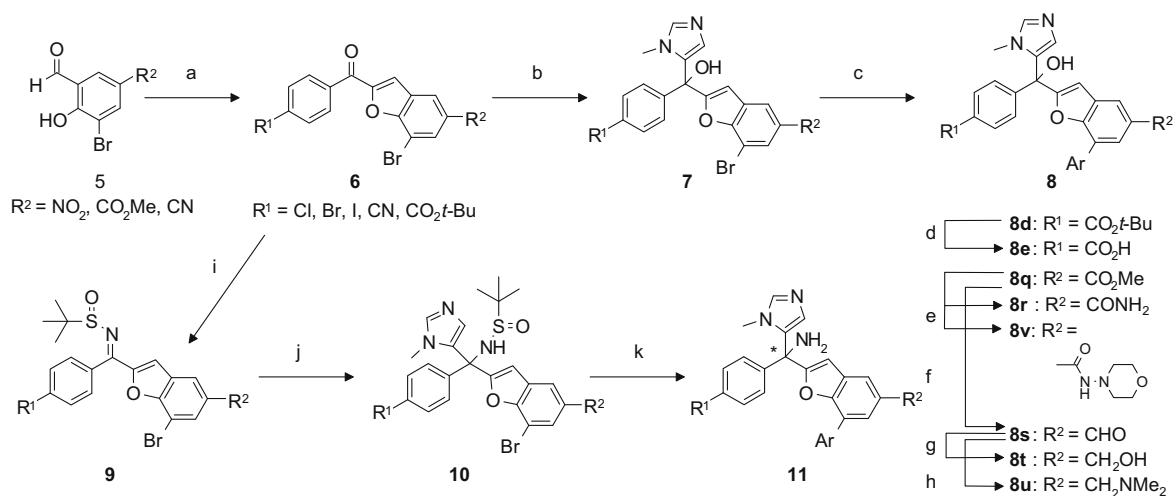


**Figure 1.** Modification of tipifarnib from core structures **1** through **3** to give benzofuran derivative (**4**).

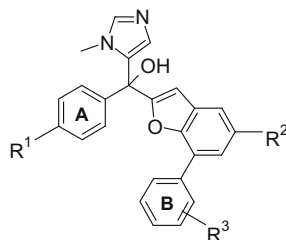
\* Corresponding author. Tel.: +81 467 47 6046; fax: +81 467 45 6824.

E-mail address: [sakaitanimsh@chugai-pharm.co.jp](mailto:sakaitanimsh@chugai-pharm.co.jp) (M. Sakaitani).



**Scheme 1.** Reagents and conditions: (a) 4-substituted phenacyl bromide,  $\text{K}_2\text{CO}_3$ ,  $\text{CH}_3\text{CN}$ , reflux, 1 h, 36–80%; (b) 1-methyl-2-TES-imidazole,  $n\text{-BuLi}$ , THF,  $-78^\circ\text{C}$ , 55–81%; (c)  $\text{ArB(OH)}_2$ ,  $\text{Pd}_2(\text{dba})_3$ ,  $\text{PPh}_3$ ,  $\text{Na}_2\text{CO}_3$ , toluene/MeOH/ $\text{H}_2\text{O}$ ,  $80^\circ\text{C}$ , 17–97%; (d) TFA/ $\text{CH}_2\text{Cl}_2$ , rt, 1 h, 73%; (e) i— $\text{LiOH}$ , THF/ $\text{H}_2\text{O}$ , 46%; ii— $\text{WSCI}$ , HOBt, DIPEA, appropriate amine, THF, 51% for **8r**, 58% for **8v**; (f) i— $\text{LiOH}$ , THF, rt, ii— $\text{HNMeOMe}$ ,  $\text{WSCI}$ , HOBt, DIPEA, DMF, rt, 56%, (iii) LAH, THF,  $-78^\circ\text{C}$ , 96%; (g)  $\text{NaBH}_4$ , MeOH, rt, 1.5 h, 90%; (h) dimethylamine,  $\text{NaB(OAc)}_3\text{H}$ , AcOH, THF, rt, 72%; (i) 2-methyl-2-propanesulfonamide,  $\text{Ti(OEt)}_4$ , toluene,  $70^\circ\text{C}$ , 2 h, 52–70%, (j) i—1-methyl-2-TES-imidazole,  $n\text{-BuLi}$ , THF, rt, 3 h, 56–76%, ii—chiral resolution by chiral HPLC system; (k) i—2-(substituted phenyl)-[1,3,2]dioxaborinane,  $\text{Pd(PPh}_3)_4$ ,  $\text{K}_3\text{PO}_4$ , DMF,  $100^\circ\text{C}$ , 1 h, 81–98%, ii— $\text{HCl}$ , THF, rt, 60–93%.

**Table 1**  
Activity of benzofuran ( $R = \text{OH}$ ) series



Compound	$R^1$	$R^2$	$R^3$	FTase/K-ras <sup>a</sup> IC <sub>50</sub> (nM)	QG56 IC <sub>50</sub> (nM)
<b>8a</b>	Cl	$\text{NO}_2$	H	170	1885
<b>8b</b>	Br	$\text{NO}_2$	H	360	1477
<b>8c</b>	I	$\text{NO}_2$	H	360	>10000
<b>8d</b>	$\text{CO}_2\text{t-Bu}$	$\text{NO}_2$	H	>1000	6248
<b>8e</b>	$\text{CO}_2\text{H}$	$\text{NO}_2$	H	850	>10000
<b>8f</b>	$\text{NO}_2$	$\text{NO}_2$	H	30	547
<b>8g</b>	OMe	$\text{NO}_2$	H	250	4967
<b>8h</b>	CN	$\text{NO}_2$	H	6.4	1477
<b>8i</b>	CN	$\text{NO}_2$	2-F	3.3	89.5
<b>8j</b>	CN	$\text{NO}_2$	3-OMe	8.5	38.8
<b>8k</b>	CN	$\text{NO}_2$	3-CN	2.8	22.9
<b>8l</b>	CN	$\text{NO}_2$	3-Me	11	23.2
<b>8m</b>	CN	$\text{NO}_2$	3-F	6.3	145
<b>8n</b>	CN	$\text{NO}_2$	4-OMe	4	36
<b>8o</b>	CN	$\text{NO}_2$	4-CN	3.4	32.6
<b>8p</b>	CN	$\text{NO}_2$	4-F	7.2	158
<b>8q</b>	CN	$\text{CO}_2\text{Me}$	3-OMe	3.2	36.3
<b>8r</b>	CN	CONH <sub>2</sub>	3-OMe	0.9	8.2
<b>8s</b>	CN	CHO	3-OMe	2	15.2
<b>8t</b>	CN	$\text{CH}_2\text{OH}$	3-OMe	1	16.8
<b>8u</b>	CN	$\text{CH}_2\text{NMe}_2$	3-OMe	11	142
<b>8v</b>	CN		3-OMe	2.6	nt <sup>b</sup>
<b>8w</b>	Cl		H	6.4	73.6
<b>8x</b>	CN	CN	H	2.4	14.5

<sup>a</sup> Human farnesyltransferase.

<sup>b</sup> Not tested.

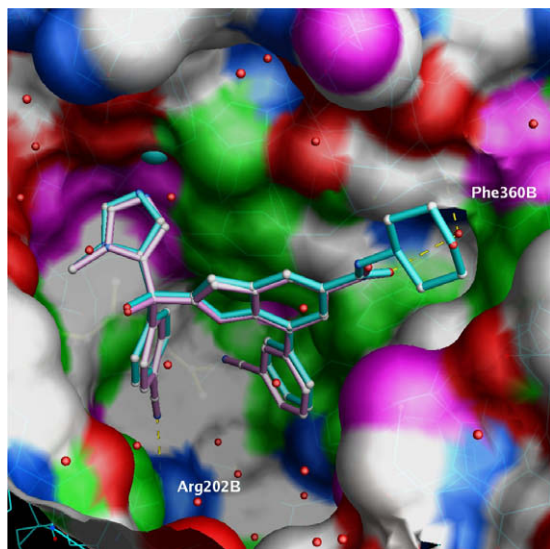
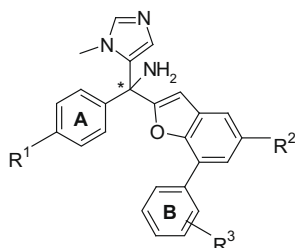


**Figure 2.** Crystal structure of FTase with **8k** (pink) and **8w** (cyan). Cyano group on A-ring of **8k** makes a hydrogen bond (3.1 Å) to Arg202B. There is a bridging water between the carbonyl oxygen on benzofuran of **8w** and amide of Phe360B.

The general synthesis of benzofuran derivatives **4** is outlined in Scheme 1. Intermediate **6** was provided from substituted benzaldehyde **5** by coupling with the appropriate phenacyl bromide under basic condition.<sup>5</sup>

Compound **7** was prepared by treatment of 1-methyl-2-TES-imidazole with *n*-BuLi followed by the addition of the appropriate **6**. A variety of aryl substituents were introduced into **7** by Suzuki coupling reaction to give biaryl **8** as a racemate ( $R^4 = \text{OH}$ ). The *t*-butyl group in **8d** was hydrolyzed to carboxylic acid (**8e**). The methyl ester group in **8q** was converted to amides (**8r** and **8v**) and an aldehyde (**8s**) which was further converted to an alcohol (**8t**) and amino derivative (**8u**). The synthesis of the other benzofuran series **11** ( $R^4 = \text{NH}_2$ ) is also described in Scheme 1. Sulfineimine **9** was prepared by tetraethyl orthotitanate mediated condensation of **6** with sulfineamide.<sup>6</sup> Arylation of **9** with 1-methyl-2-TES-imidazole-5-lithium followed by chiral resolution using an HPLC system with a chiral column afforded **10**.<sup>7,8</sup> Suzuki coupling of **10** with 2-(substituted phenyl)-[1,3,2]dioxaborinane, followed by deprotection of the *t*-butylsulfine group under acidic condition gave the desired product **11**.

**Table 2**  
Activity of benzofuran ( $R^4 = \text{NH}_2$ ) series



Compound	R <sup>1</sup>	R <sup>2</sup>	R <sup>3</sup>	Chiral	FTase/K-ras <sup>a</sup> IC <sub>50</sub> (nM)	QG56 IC <sub>50</sub> (nM)
<b>11a</b>	CN	NO <sub>2</sub>	H	S	1.5	5.9
<b>11b</b>	CN	NO <sub>2</sub>	H	R	49	206.1
<b>11c</b>	CN	NO <sub>2</sub>	3-OMe	S	0.8	1.1
<b>11d</b>	CN	CN	3-OMe	S	1.2	1.5
<b>11e</b>	CN	CN	3-CN	S	0.7	2
<b>11f</b>	CN	CN	3-F	S	1.1	2

<sup>a</sup> Human farnesyltransferase.

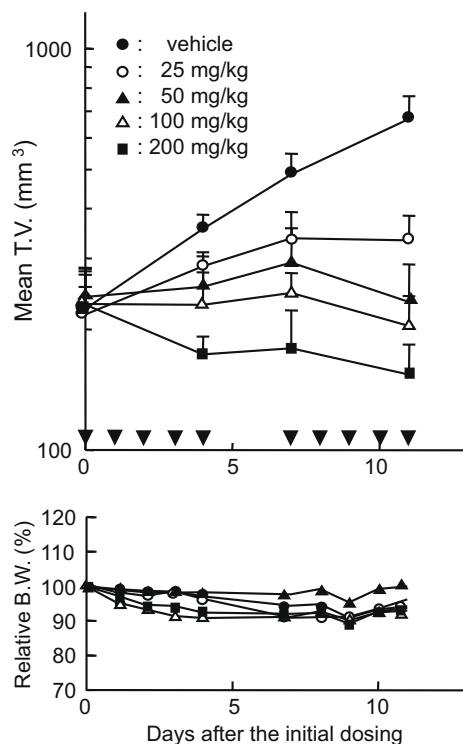


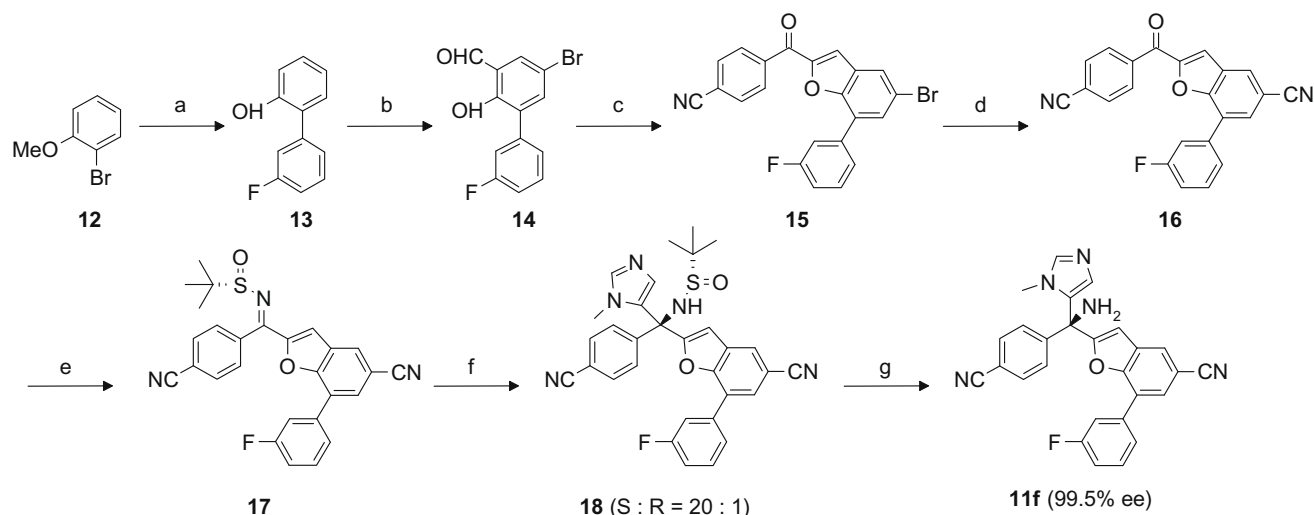
**Figure 3.** Effect of **11f** on QG56 tumor growth in mouse xenograft models. Tumor volume (TV) was measured twice/week (upper graph). Body weight (BW) was measured 5 times/week and relative BW calculated (lower graph).

The enzyme inhibitory activity (FTase/K-ras) and antiproliferative activity against human non-small cell lung carcinoma (QG56) of compounds (**8**) were evaluated.<sup>9</sup> The results from compound **8** having a hydroxyl group at the chiral center are shown in Table 1. Our first lead compound (**8a**) showed weak FTase inhibition ( $\text{IC}_{50} = 170 \text{ nM}$ ) and low antiproliferative activity ( $\text{IC}_{50} = 1885 \text{ nM}$ ). Introduction of a cyano group (**8h**) or a nitro group (**8f**) on the A-ring resulted in significant increase of enzyme inhibitory activities (6.4 and 30 nM respectively). Replacement of the chlorine atom with another halogen (**8b** and **8c**), *t*-butylester (**8d**), carboxylic acid (**8e**), or methoxy (**8g**) resulted in reduction of enzyme inhibitory activity (from 250 to 1000 nM). Further modification of the substituent R<sup>3</sup> in the compound (**8h**) was carried out. The compound having a 3-CN group (**8k**) showed potent enzyme inhibitory activity (2.8 nM) and antiproliferative activity (23 nM). The X-ray crystal structure of FTase complexed with **8k** shown in Figure 2 suggests that the hydrogen bonding between the cyano group on the A-ring and Arg202B improves the enzyme inhibitory activity.<sup>10</sup> No obvious interaction of the cyano group on the B-ring with the enzyme was seen. In fact, all the compounds having small substituents on the B-ring (**8i–p**) showed similar FTase inhibition (2.8–11 nM) compared with a non-substituted phenyl (**8h**, 6.4 nM) but exhibited improved antiproliferative activity against QG56 cells (23–158 nM). The effects of the substituent R<sup>2</sup> on the benzofuran ring of compound **8** are summarized in Table 1 (note **8q–v**). Interestingly, replacement of the nitro group

**Table 3**  
Pharmacokinetics of **11f** in mice<sup>a</sup>

	Cmax (μg/mL)	AUC <sub>0–24 h</sub> (μg h/mL)	CL/F (mL/min/kg)	t <sub>1/2</sub> (h)	BA (%)
IV 25 mg/kg	—	15.4	27.0	1.2	—
PO 25 mg/kg	1.57	10.2	40.8	2.4	66
PO 100 mg/kg	5.01	31.3	41.0	12.3	51

<sup>a</sup> Vehicle: 0.06 M HCl, 0.44% CMC distilled water.



**Scheme 2.** Reagents and conditions: (a) *i*-4-fluoroboronic acid, Pd(OAc)<sub>2</sub>, PPh<sub>3</sub>, Na<sub>2</sub>CO<sub>3</sub>, MeOH, reflux, 14 h, ii-BBr<sub>3</sub>, CH<sub>2</sub>Cl<sub>2</sub>, 0 °C to rt, 87%; (b) *i*-paraformaldehyde, MgCl<sub>2</sub>, Et<sub>3</sub>N, THF, reflux, 2 h, ii-NBS, CHCl<sub>3</sub>, reflux, 2 h; (c) 4-cyanophenacyl bromide, K<sub>2</sub>CO<sub>3</sub>, CH<sub>3</sub>CN, reflux, 1 h, 78% from 13; (d) Zn(CN)<sub>2</sub>, Pd(PPh<sub>3</sub>)<sub>4</sub>, DMF, 100 °C, 4 h, 90%; (e) (*S*)-2-methyl-2-propanesulfonamide, Ti(OEt)<sub>4</sub>, toluene, 70 °C, 2 h, 90%; (f) 5-bromo-*N*-methyl-imidazole, EtMgBr, CH<sub>2</sub>Cl<sub>2</sub>, THF, rt, 3 h, 80%; (g) *i*-4-M HCl in THF, rt, 1 h; ii-crystallization from H<sub>2</sub>O/MeOH/EtOH, 70%.

with a carbonyl function such as a methylester (**8q**) amide (**8r**, **8v**), or CHO (**8s**), showed 3- to 8-fold higher enzyme inhibitory activity (0.9–3.2 nM) than **8j** (8.5 nM). X-ray crystal structure of FTase with **8w** (Fig. 2) revealed a bridging water molecule forming a hydrogen bonding between the oxygen atom of the carbonyl in the substituent R<sup>2</sup> on the benzofuran and the amide backbone of the Phe360B.<sup>10</sup> Thus, the compounds with a carbonyl moiety have strong activity against FTase (**8a** vs. **8w**). Compounds **8t** and **8x** also showed strong enzyme inhibitory activity (1.0 and 2.4 nM, respectively, with FTase). These results indicate that not only a carbonyl moiety but also a hydrogen bond accepting (HBA) group is essential to increase the enzyme inhibitory activity. **8x** has strikingly strong cellular activity (14.5 nM) even though it has no substituent (R<sup>3</sup> = H) on the B-ring.

The results from *in vitro* evaluation of compound **11** (R<sup>4</sup> = NH<sub>2</sub>) are shown in Table 2. With regard to the stereochemistry of the chiral amino group, the nitro derivative with an (*S*)-configuration (**11a**) showed 33 times higher enzyme inhibitory activity than the corresponding (*R*)-isomer (**11b**). Furthermore, in the (*S*)-isomer series, replacement of the nitro group (R<sup>2</sup>) with a cyano group and the introduction of favorable substituents (R<sup>3</sup>) on the B-ring led us to identify compounds (**11d–f**) showing potent inhibitory activities against both FTase (0.7–1.2 nM) and QG56 cells (1.5–2.0 nM) (Table 2).

The antitumor activity of compounds **11c–f** was evaluated with a human cancer xenograft model showing potent antitumor activity *in vivo*. The *in vivo* efficacy of **11f** in human non-small cell lung carcinoma (QG56) xenograft in mice is shown in Figure 3.<sup>11</sup> **11f** was administered 5 times a week for 2 weeks orally at doses of 25–200 mg/kg per day. **11f** showed strong tumor regression with no noticeable body weight loss at the dose of 200 mg/kg.

After evaluation of several parameters including solubility, biological stability, and pharmacokinetics we identified **11f** as a clinical candidate. The pharmacokinetics data in mice of **11f** is presented in Table 3. **11f** was administered intravenously at dose of 25 mg/kg and orally at doses of 25 and 100 mg/kg. Oral bioavailability of **11f** was more than 50% and AUC was increased dose-dependently. It has been confirmed that there was a good correlation between AUC and tumor growth inhibition *in vivo*.

The chiral synthesis of **11f** was established by modification of the synthetic route shown in Scheme 1 and outlined in Scheme 2. The most dramatic improvement was made in the diastereose-

lective addition of an imidazole moiety into chiral sulfineimine **17** to give **18**. Although the addition of 1-methyl-2-TES-imidazole treated with *n*-BuLi resulted in low diastereoselectivity (S:R = 2:1), the Grignard condition, treated by EtMgBr, showed dramatically improved selectivity (S:R = 20:1). This new synthetic process has significant advantage for further scale-up synthesis because all the intermediates can be purified by crystallization without using column chromatography.<sup>12</sup>

In summary, we discovered a series of benzofuran compounds showing potent FTase inhibitory activity. A cyano group at the para-position of the A-ring (R<sup>1</sup> position) showed excellent FTase inhibition. Substituent of the functional group at the B-ring (R<sup>3</sup> position) increased antiproliferative activity against human cancer cell lines. Introduction of an HBA group at the R<sup>2</sup> position resulted in improved inhibitory activities both in enzyme and cellular assays. X-ray crystal structure of FTase with **8k** and **8w** revealed important hydrogen bonding of (1) the cyano group at the R<sup>1</sup> position of **8k** with Arg202 and (2) the carbonyl group at the R<sup>2</sup> position of **8w** with a water molecule bound to the protein. Compound **11f**, a clinical candidate, showed strong tumor regression in the QG56 human NSCLC xenograft model with no noticeable body weight loss. **11f** also showed good pharmacokinetics profile in mice. Furthermore, we established diastereoselective synthesis of **11f** applicable to large scale synthesis.

## Acknowledgments

We are grateful to Mr. Toshihiko Fujii and Mr. Kiyooki Sakata for *in vitro* biological assays. We also thank Dr. Satoshi Sogabe for analysis of the X-ray crystallographic data and Dr. Kazunao Masubuchi and Ms. Miyuki Asai for synthesis of the compounds. We thank Drs. Mamoru Suzuki and Noriyuki Igarashi and Prof. Noriyoshi Sakabe at the Photon Factory for assistance with the beam line station (BL-6B).

## References and notes

- (a) Clarke, S. *Annu. Rev. Biochem.* **1992**, *61*, 355; (b) Cox, A. D.; Der, C. J. *Crit. Rev. Oncog.* **1992**, *3*, 365; (c) Gibbs, J. B. *Cell* **1991**, *65*, 1; (d) Newman, C. M. H.; Magee, A. I. *Biochim. Biophys. Acta* **1993**, *1155*, 79; (e) Schafer, W. R.; Rine, J. *Annu. Rev. Genet.* **1992**, *26*, 209.
- Tamanoi, F.; Kato-Stankiewicz, J.; Jiang, C.; Machado, I.; Thapar, N. *J. Cell. Biochem. Suppl.* **2001**, *37*, 64.

3. (a) Leonard, D. M. *J. Med. Chem.* **1997**, *40*, 2971; (b) Sebti, S. M.; Hamilton, A. D. *Drug Discov. Today* **1998**, *3*, 26.
4. Jabbour, E.; Kantarjian, H.; Cortes, J. *Expert Opin. Investig. Drugs* **2007**, *16*, 381.
5. Stille, J. R.; Ward, J. A.; Leffelman, C.; Sullivan, K. A. *Tetrahedron Lett.* **1996**, *37*, 9353.
6. Cogan, D. J.; Liu, G.; Kim, K.; Bradley, B. J.; Backes, J.; Ellman, J. A. *J. Am. Chem. Soc.* **1998**, *120*, 8011.
7. Carpenter, A. J.; Chadwick, D. J. *Tetrahedron* **1986**, *42*, 2358.
8. Prepared diastereomers were separated and purified by chiral column chromatography over DAICEL CHIRACEL OD (eluent: hexane/2-propanol 1:1).
9. Assay methods described in: Sakaitani, M.; Masubuchi, K.; Kohchi, M.; Hyoudoh, I.; Asoh, K.; Asai, M. WO Patent 04/037816, 2004.
10. Crystals of rat FTase with compounds were obtained within a week under the crystallization condition of 10% (w/v) PEG 6000, 0.2 M Mg acetate, 0.1 M Na acetate buffer (pH4.5) at 4 °C. The structures in complex with compounds **8k** and **8w** were solved at 2.6 and 2.4 Å, respectively, and their coordinates have been deposited in the Protein Data Bank under the access codes **2ZIS** and **2ZIR**.
11. Materials and methods human tumor cell line: The QG56 human non-small cell lung cancer cell line was cultured in RPMI-1640 medium supplemented with 10% (v/v) fetal bovine serum. Animals: 5-week-old male athymic nude mice were subjected to the experiment. Compound **11f** was dissolved in 0.06 M HCl, 0.44% CMC distilled water. Determination of antitumor activities: The in vivo evaluation procedure for anticancer drugs was based on the National Cancer Institute (NCI) guidelines. A single cell suspension of QG56 ( $5.0 \times 10^6$  cells per mouse) was inoculated subcutaneously into the right flank of each mouse. The tumor volume was estimated from two-dimensional measurements using the equation  $ab^2/2$ , where  $a$  and  $b$  represent tumor length and width, respectively. Drug administration was initiated on the day of grouping (day 0). **11f** was administered orally once a day from days 0 to 4 and days 7 to 11.
12. **11f** was analyzed by chiral column chromatography over DAICEL CHIRALPAK® AS (eluent: hexane/ethanol, 4:1) to determine enantiomeric excess.